Available online at www.sciencedirect.com
ScienceDirect
Journal of Photochemistry and Photobiology A: Chemistry 194 (2008) 49–58
Journal of Photochemistry and Photobiology A:Chemistry
www.elsevier.com/locate/jphotochem

Synthesis, characterization, cytotoxic activity and DNA-binding properties of the Ln(III) complexes with ethylenediiminobi(6-hydroxychromone-3-carbaldehyde) Schiff-base

Bao-dui Wang [a], Zheng-Yin Yang [a,*], Dong-dong Qin [a], Zhong-Ning Chen [b]

[a] *College of Chemistry and Chemical Engineering and State Key Laboratory of Applied Organic Chemistry, Lanzhou University, Lanzhou 730000, PR China*

[b] *Fujian Institute of Research on The Structure of Matter, Chinese Academy of Sciences, Fuzhou 350002, PR China*

Received 6 April 2007; received in revised form 1 July 2007; accepted 16 July 2007
Available online 2 August 2007

Abstract

A new ligand, ethylenediiminobi(6-hydroxychromone-3-carbaldehyde) Schiff-base (L), was prepared by condensation of 6-hydroxy-3-carbaldehyde chromone (CDC) with ethylenediamine. Its three rare earth complexes have been synthesized and characterized on the basis of elemental analyses, molar conductivities, mass spectra, ^{1}H NMR, thermogravimetry/differential thermal analysis (TG-DTA), UV–vis spectra, fluorescence spectra and IR spectra. The general formula of the complexes is $[LnL\cdot(NO_3)_2]\cdot NO_3$ [Ln = Sm (**1**), Eu (**2**), La (**3**)]. Complexes **1**, **2** and **3**, and ligand **L** were subjected to biological tests in vitro using HepG2 cancer cell lines. Ligand showed significant cytotoxic activity against HepG2cancer cell lines. Spectrometric titration, ethidium bromide displacement experiments and viscosity measurements indicate that Sm(III) and Eu(III) complexes strongly bind with calf thymus DNA, presumably via an intercalation mechanism. The intrinsic binding constants of complexes **1** and **2**, and ligand with DNA were 9.28×10^6, 8.40×10^6 and 4.88×10^6 M^{-1} through fluorescence titration data, respectively.

Keywords: Ethylenediiminobi(6-hydroxychromone-3-carbaldehyde) Schiff-base; Rare earth complexes; DNA binding

1. Introduction

The study on the interaction of small molecules, such as metal, drugs, organic dyes with DNA is one of interest because it is important in the design of new and more efficient drugs targeted to DNA [1,2]. A variety of small molecules are bound by electrostatic interaction with the exterior sugar–phosphate backbone or by hydrophobic interaction along the minor groove of DNA or by intercalative interaction between the stacked bases pairs of native DNA from the major groove [2,3]. Among the three modes, the most effective mode of the drugs targeted to DNA is intercalating binding [4]. Thus, the research of interaction of intercalating agent with DNA is vital. However, during the past decade, the interaction of polypyridyl compounds and their complexes with DNA has attracted much attention [5–9].

Many clinically successful anticancer drugs were themselves either naturally occurring molecules or have been developed from their synthetic analogs. Great interest is currently being paid to natural products for their interesting anticancer activities. Flavonoids are a broadly distributed class of naturally occurring pigments present in vascular plants, and are responsible for most of the colors in nature. These natural products are potentially antibacterial, anticancer, antioxidant, anti-inflammatory, and antiallergenic agents since they stimulate or inhibit a

Abbreviations: CT-DNA, calf thymus DNA; L, ethylenediiminobi(6-hydroxychromone-3-carbaldehyde) Schiff-base; Tris, Tris(hydroxymethyl)-aminomethane; NMR, nuclear magnetic resonance; EB, ethidium bromide; CDC, 6-hydroxy-3-carboxaldehydes chromone; UV-vis, ultraviolet and visble; TG-DTA, thermogravimetry/differential thermal analysis; DMF, *N*,*N*-dimethyl formamide; SDS, $CH_3(CH_2)_{11}OSO_3Na$; SOD, superoxide dismutaes; MTT, 3-(4,5-dimethyl-2-thiazoyl)-2,5-diphenyl-2*H*-tetrazolium bromide

* Corresponding author. Fax: +86 931 8912582.
E-mail address: yangzy@lzu.edu.cn (Z.-Y. Yang).

1010-6030/$ – see front matter © 2007 Published by Elsevier B.V.
doi:10.1016/j.jphotochem.2007.07.024

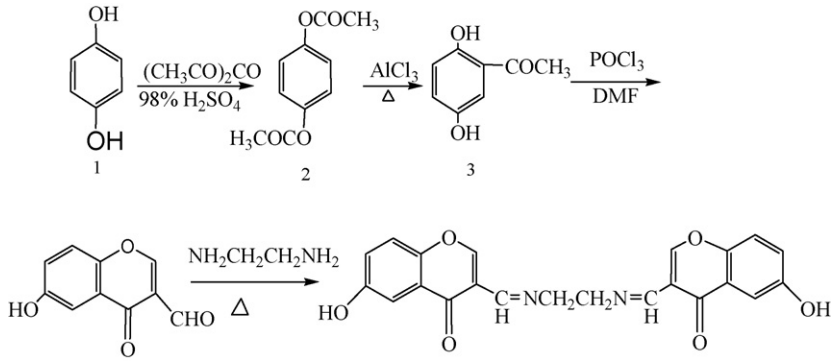

Fig. 1. Preparation route of the ligand.

wide variety of enzyme systems as pharmacological agents [10–15].

Biological activity and also number of other applications resulted in strongly increasing interest for lanthanides in the last decade [16–20]. One of the most studied applications is usage of the lanthanide/small molecule complexes to address DNA/RNA by non-covalent binding and/or cleavage [21–24]. In our research, we have found that the rare earth complexes of flavane benzoyl hydrazone have certain antioxidant and cytotoxic activity, and can bind to CT-DNA by intercalation [24–26].

As a part of our continuing research DNA binding model of the flavone benzoyl hydrazone and its complexes, in this paper, we synthesized a new ligand, ethylenediiminobi(6-hydroxychromone-3-carbaldehyde) Schiff-base (Fig. 1), and its rare earth complexes. We described a comparative study of the interactions of Sm(III) and Eu(III) complexes, and ligand with CT-DNA using UV–vis, fluorescence and viscosity measurements for the first time. Information obtained from this study will be helpful to the understanding of the mechanism of interactions of chromone hydrazones and their complexes with nucleic acids, and should be useful in the development of potential probes of DNA structure and conformation and new therapeutic regents for some diseases.

2. Experimental

2.1. Chemicals

Acetic anhydride, hydroquinone were produced in China. The rare earth (III) nitrates were derived from their oxide (99.9%) acquired from Nong Hua (PRC).

2.2. DNA sample

Calf thymus DNA (CT-DNA) was obtained from Sigma Chemicals Co. (USA) and used as received. A stock solution of CT-DNA was prepared and stored in 5 mM Tris–HCl buffer at pH 7.1. The concentration of CT-DNA solutions was determined spectrophotometrically using the reported molar absorptivity of $\varepsilon_{259\,nm} = 1.31 \times 10^4\,M^{-1}\,cm^{-1}$ [27] and the results were expressed in terms of base-pair equivalents per cubic decimeter. A solution of CT-DNA (ca. 10^{-5} M in base pair, bp) in Tris–HCl buffer gave a ratio of UV absorbance at 260 and 280 nm, $A_{260}/A_{280} \geq 1.9$ [28], indicating that the CT-DNA was sufficiently free from protein.

2.3. Instrumentation

Carbon, hydrogen, and nitrogen were analyzed on an Elemental Vario EL analyzer. The metal contents of the complex were determined by titration with EDTA. Infrared spectra (4000–400 cm^{-1}) were determined with KBr disks on a Therrno Mattson FTIR spectrometer. The UV–vis spectra were recorded on a Varian Cary 100 Conc spectrophotometer. ^{1}H NMR spectra were measured on a Varian VR 300-MHz spectrometer, using TMS as a reference in DMSO-d_6. Mass spectra were performed on a VG ZAB-HS (FAB) instrument and electrospray mass spectra (ESI-MS) were recorded on a LQC system (Finngan MAT, USA) using CH3OH as mobile phase. The fluorescence spectra were recorded on a Hitachi RF-4500 spectrofluorophotometer.

2.4. Preparation of ligand (L)

CDC was prepared according to the literature methods [29]. An ethanol solution containing ethylenediamine (0.06 g, 10 mmol) was added dropwise to another ethanol solution containing CDC (1.90 g, 10 mmol). The mixture was stirred for 2 h at room temperature and a yellow precipitate was formed. The precipitate was collected by filtration and washed with ethanol. Recrystallization from 1:1 (v/v) DMF/H_2O gave the ligand (L), which was dried in a vacuum. Yield: 90%. FAB-MS: $m/z = 405$ $[M+H]^+$. Anal. Calcd. (%) for $C_{22}H_{16}N_2O_6$: C, 65.50; H, 1.48; N, 5.95. Found: C, 65.12; H, 1.32; N, 5.74. ^{1}H NMR (DMSO-d_6 300 MHz): δ 10.04 (2H, s, OH), 9.15 (2H, s, CH=N), 7.20–6.77 (8H, m, PhH, 2, 5, 7, 8-H), 3.47 (4H, s, $-CH_2CH_2-$). IR for ligand (cm^{-1}): $\nu_{C=O}$: 1649, $\nu_{C=N}$: 1557, ν_{C-O-C}: 1295, ν_{OH}: 3421. U_{max} (nm): 200, 223, 258, 325.

2.5. Preparation of complexes

The ligand (1.0 mmol, 0.403 g) and the Sm(III) nitrate (1.0 mmol, 0.4482 g) were added together in ethanol (10 mL). The mixtures were stirred at 60 °C for 24 h. A white precipitated, the Sm(III) complex, was separated from the solution by suction filtration, purified by washing several times with ethanol, and dried for 24 h in a vacuum. Eu(III) and La(III) complexes were

prepared by the same way. Anal. Calcd. (%) for Sm(III) complex $C_{22}H_{16}N_5O_{15}$ Sm (%): C, 35.46 (35.65); H, 2.36 (2.16); N, 9.78 (9.45); Sm, 20.12 (20.13). Λ_m ($S\,cm^2\,mol^{-1}$): 101. IR (cm^{-1}): $\nu_{C=O}$: 1643, $\nu_{C=N}$: 1525, ν_{C-O-C}: 1281, ν_{OH}: 3384, ν_{NO_3}: 1487, 1395, 1325, 1068, 838. U_{max} (nm): 204, 251, 321. Thermal analyses: $T_{Decomp.}$ (°C): 342, 545. Residue Calcd. (%) 23.19 (23.55). ESI-MS [CH_3OH, *m/z*]: 739.0 $\{[SmL\cdot(NO_3)_2]\cdot NO_3–H\}^-$, 678.8 $\{SmL\cdot(NO_3)_2\}\cdot NO_3–NO_3^-\}^+$, 617 $\{SmL\cdot(NO_3)_2\}\cdot NO_3–2NO_3^-–H\}^+$ and 308 $\{SmL\cdot(NO_3)_2\}\cdot NO_3–2NO_3^-\}^{2+}$. Anal. Calcd. (%) for Eu(III) complex $C_{22}H_{16}N_5O_{15}$ Eu (%): C, 35.67 (35.58); H, 2.31 (2.16); N, 9.89 (9.43); Eu, 20.14 (20.48). Λ_m ($S\,cm^2\,mol^{-1}$): 103. IR (cm^{-1}): $\nu_{C=O}$: 1644, $\nu_{C=N}$: 1525, ν_{C-O-C}: 1282, ν_{OH}: 3383, ν_{M-O}: 578, ν_{NO_3}: 1483, 1395, 1325, 1065, 838. U_{max} (nm): 203, 251, 318. Thermal analyses: $T_{Decomp.}$ (°C): 342, 545. Residue Calcd. (%) 23.19 (23.55). ESI-MS [CH_3OH, *m/z*]: 739.6 $\{[EuL\cdot(NO_3)_2]\cdot NO_3–H\}^-$, 678 $\{EuL\cdot(NO_3)_2\}\cdot NO_3–NO_3^-\}^+$, 619 $\{EuL\cdot(NO_3)_2\}\cdot NO_3–2NO_3^-–H\}^+$ and 308 $\{EuL\cdot(NO_3)_2\}\cdot NO_3–2NO_3^-\}^{2+}$. Anal. Calcd. (%) for La(III) complex $C_{22}H_{16}N_5O_{15}$ La (%): C, 36.57 (36.41); H, 2.49 (2.19); N, 9.06 (9.60); La, 20.14 (20.48). Λ_m ($S\,cm^2\,mol^{-1}$): 102. IR (cm^{-1}): $\nu_{C=O}$: 1644, $\nu_{C=N}$: 1525, ν_{C-O-C}: 1284, ν_{OH}: 3383, ν_{M-O}: 578, ν_{NO_3}: 1483, 1395, 1325, 1065, 838. U_{max} (nm): 203, 251, 318. Thermal analyses: $T_{Decomp.}$ (°C): 342, 545. Residue Calcd. (%) 20.19 (19.06). ^1H NMR (DMSO-d_6 300 MHz): δ 10.11 (2H, s, OH), 8.64 (2H, s, CH=N), 8.468 (2H, s, 2-H) 7.46–6.70 (6H, m, PhH, 5, 7, 8-H), 3.76 (4H, s, $–CH_2CH_2–$). ESI-MS [CH_3OH, *m/z*]: 727.6 $\{[LaL\cdot(NO_3)_2]\cdot NO_3–H\}^-$, 666 $\{LaL\cdot(NO_3)_2\}\cdot NO_3–NO_3^-\}^+$, 613 $\{LaL\cdot(NO_3)_2\}\cdot NO_3–2NO_3^-–H\}^+$ and 307 $\{LaL\cdot(NO_3)_2\}\cdot NO_3–2NO_3^-\}^{2+}$.

2.6. An absorption titration

Absorption titration experiment was performed with fixed concentrations of the drugs (10 μM) while gradually increasing concentration of DNA. While measuring the absorption spectra, an equal amount of DNA was added to both compound solution and the reference solution to eliminate the absorbance of DNA itself.

2.7. Fluorescence spectra

To compare quantitatively the affinity of the compound bound to DNA, the intrinsic binding constants K_b of the two compounds to DNA were obtained by the luminescence titration method. Fixed amounts of compound were titrated with increasing amounts of DNA, over a range of DNA concentrations from 0 to 20.0 μM. An excitation wavelength of 320 nm was used, and total fluorescence emission intensity was monitored at 449 nm for complexes and ligand. The concentration of the bound compound was calculated using Eq. (1) [30]:

$$C_b = C_t\left[\frac{(F - F^0)}{(F^{max} - F^0)}\right]$$

where C_t is the total compound concentration; F the observed fluorescence emission intensity at given DNA concentration; F^0 the intensity in the absence of DNA, and F^{max} is the fluorescence of the totally bound compound. Binding data were cast into the form of a Scathchard plot [31] of r/C_f versus r, where r is the binding ratio, $C_b/[DNA]_t$ and C_f is the free ligand concentration. All experiments were conducted at 20 °C in a buffer containing 5 mM Tris–HCl (pH 7.1) and 50 mM NaCl concentrations.

Further support for complexes **1** and **2**, and ligand binding to DNA by intercalation mode is given through the emission quenching experiment. EB is a common fluorescent probe for DNA structure and has been employed in examinations of the mode and process of metal complex binding to DNA [32]. A 2-mL solution of 10 μM DNA and 0.33 μM EB (at saturating binding levels [33]) was titrated by 5–30 μM complexes **1** and **2**, and ligand (λ_{ex} = 500 nm, λ_{em} = 520.0–650.0 nm).

According to the classical Stern–Volmer equation [34]:

$$\frac{F_0}{F} = K_q[Q] + 1$$

where F_0 is the emission intensity in the absence of quencher, F the emission intensity in the presence of quencher, K_q the quenching constant, and $[Q]$ is the quencher concentration. The shape of Stern–Volmer plots can be used to characterize the quenching as being predominantly dynamic or static. Plots of F_0/F versus $[Q]$ appear to be linear and K_q depends on temperature.

2.8. Viscosity measurements

Viscosity experiments were conducted on an Ubbdlodhe viscometer, immersed in a thermostated water-bath maintained to 25.0 °C. Titrations were performed for the complexes **1** and **2** (1–5 μM), and each compound was introduced into DNA solution (5 μM) present in the viscometer. Data were presented as $(\acute{\eta}/\acute{\eta}_0)^{1/3}$ versus the ratio of the concentration of the compound and DNA, where $\acute{\eta}$ is the viscosity of DNA in the presence of compound and $\acute{\eta}_0$ is the viscosity of DNA alone. Viscosity values were calculated from the observed flow time of DNA containing solution corrected from the flow time of buffer alone (t_0), $\acute{\eta} = t - t_0$ [35,36].

2.9. Cytotoxicity assay

Tumor cell lines used in this work were grown in a RPMI-1640 medium supplement with 10% (v/v) calf serum, 2 $mmol^{-1}$ glutamine, 100 U mL^{-1} penicillin (U = 1 unit of activity), and 100 μg mL^{-1} streptomycin (GIBCO, Grand Island, NY) at 310 K under 5% CO_2. Cells in 100 μL culture mediums were seeded into 96-well plates (Falcon, CA).

For HepG2 cells, the growth inhibition was analyzed by the SRB (sulforthodamine B) assay [37]. Simply, following the treatment of the cells with the compound to be tested for 72 h, the cell cultures were then fixed with 10% trichloroacetic acid and incubated for 60 min at 277 K. The plates were then washed and dried, following which a SRB solution (0.4%, w/v, in 1% acetic acid) was added and the culture was incubated for an additional 15 min. After the plates were washed and dried, the bound stain was solublized with Tris buffer, and

the optical densities were read by the plate reader at 515 nm. The growth inhibitory rate of treated cells was calculated by $((OD_{control} - OD_{test})/OD_{control}) \times 100\%$.

3. Results and discussion

The complexes were prepared by direct reaction of ligand with the appropriate mole ratios of Sm(III), Eu(III) and La(III) nitrate in ethanol. The yields were good to moderate. The desired complexes were separated from the solution by suction filtration, purified by washing several times with ethanol. The complexes are air stable for extended periods and soluble in methanol, DMSO, and DMF; slightly soluble in ethanol and water; insoluble in benzene and diethyl ether. The complexes have been unambiguously characterized through mass spectral analysis. The mass spectrum of complex **1** shows peaks at *m/z* of 740, 678 and 619 which can be assigned to the ion pair $\{[SmL{\cdot}(NO_3)_2]{\cdot}NO_3{-}H\}^-$, $\{SmL{\cdot}(NO_3)_2\}{\cdot}NO_3{-}NO_3^-\}^+$ and $\{SmL{\cdot}(NO_3)_2\}{\cdot}NO_3{-}2NO_3^-{-}H\}^+$, respectively. Similarly, the mass spectrum of complex **2** also shows peak at *m/z* of 741, 678, 619 and 308 which can be assigned to the ion pair $\{[EuL{\cdot}(NO_3)_2]{\cdot}NO_3{-}H\}^-$, $\{EuL{\cdot}(NO_3)_2\}{\cdot}NO_3{-}NO_3^-\}^+$, $\{EuL{\cdot}(NO_3)_2\}{\cdot}NO_3{-}2NO_3^-{-}H\}^+$ and $\{EuL{\cdot}(NO_3)_2\}{\cdot}NO_3{-}2NO_3^-\}^{2+}$ The molar conductivities of the complexes are around 101–103 S cm^2 mol^{-1} in DMF, showing that complexes are 1:1 electrolytes [38]. In the ^{1}H NMR, the –OH group and 2-H of the complex shifts downfield compared to that of the free ligand. These changes in the chemical shifts are due to the coordination of the oxygen of carbonyl of the ligand. The elemental analyses, mass spectrum and molar conductivities show that formulas of the complexes conform to $[LnL{\cdot}(NO_3)_2]{\cdot}NO_3$.

3.1. IR spectra

The ν(C=O) vibration of the free ligand is at 1649; for the complexes these peaks shift to 1643 cm^{-1} or so. The Ln(III) complex spectra showed a new band, compared to the spectrum of the free ligand, at 578 cm^{-1}. It was assigned to metal-oxygen stretching vibrations, in agreement with literature data [23,29,39]. For the ligand, the ν(OH) appears at 3421 cm^{-1}; this band for the complexes shifts to 3384 cm^{-1} or so. The band at 1295 cm^{-1} for the free ligand is assigned to the ν(C–O–C) stretch, which shifts to 1282 cm^{-1} for its complexes. The –OH group and 2-H of the complex shifts downfield compared to that of the free ligand. All of these observations demonstrate that the oxygen of carbonyl has formed a coordinative bond with the rare earth ions. The band at 1557 cm^{-1} for the free ligand is assigned to the ν(C=N) stretch, which shifts to 1525 cm^{-1} for its complexes. Weak bands at 436 cm^{-1} are assigned to ν(M–N). These shifts and the new band further confirm that the nitrogen of the imino-group bonds to the rare earth ions [24,29]. The absorption bands of the coordinated nitrates were observed at about 1487 (ν_{as}) and 838 (ν_s) cm^{-1}. The ν_3(E′) free nitrates appear at 1395 cm^{-1} in the spectra of the complexes. In addition, the separation of the two highest frequency bands $|\nu_4{-}\nu_1|$ is approximately 158 cm^{-1}, and accordingly the coordinated NO_3^- ion in the complex is a bidentate ligand [24,29].

Table 1
Fluorescence data of the Eu(III) complex at room temperature

State	Slit (nm)	λ_{ex} (nm)	λ_{em} (nm)	[a]RFI	Assignment
Complexes 2					
Solid	1	344	579.4	83.63	$^5D_0 \rightarrow {}^7F_0$
			590.8	227.9	$^5D_0 \rightarrow {}^7F_1$
			616.2	469.8	$^5D_0 \rightarrow {}^7F_2$
Acetone			591.2	162.3	$D_0 \rightarrow {}^7F_1$
			615.6	305.5	$^5D_0 \rightarrow {}^7F_2$
Acetonitrilet	5.0	379	615	125.6	$^5D_0 \rightarrow {}^7F_2$
$CHCl_3$			614.2	101.9	$^5D_0 \rightarrow {}^7F_2$
DMF			614	71.65	$^5D_0 \rightarrow {}^7F_2$
DMSO			614	67.64	$^5D_0 \rightarrow {}^7F_2$

[a] RFI is relative fluorescence intensity.

3.2. UV spectra

The study of the electronic spectra in the ultraviolet and visible ranges for the complexes **1** and **2**, and the ligand were carried out in a buffer solution. The electronic spectra of ligand had a strong band at λ_{max} = 200 nm, two medium band at λ_{max} = 223 and 258 nm and a weak band at λ_{max} = 325 nm. In the complexes, the band at 223 disappeared, and the other three at 200, 223 and 325 nm are shifted to 204, 251 and 318 nm or so. These indicate that complexes are formed.

3.3. Thermal analyses

The complexes begin to decompose at 342 °C or so and there are three exothermic peaks appear around 342–547 °C. The corresponding TG curves show a series of weight loss. Under 200 °C, there are no endothermic peak and no weight loss on corresponding TG curves. It indicates that there are no crystal or coordinate solvent molecules. While being hated to 800 °C, the complexes become their corresponding oxides. The residues are in accordance with calculation.

3.4. Fluorescence studies

The fluorescence characteristics of the europium complex in solid state and in $CHCl_3$, acetone, acetonitrilet, DMF and DMSO solutions (concentration: 1.0×10^{-4} M) are listed in Table 1. It can be seen that the Eu(III) complex shows strong emission when excited with 425 nm radiation in the solid state (Fig. 2). Fluorescence arises from ligand-to-cation energy transfer, mainly from the lowest resonance level. The most intensity ratio value η ($^5D_0 \rightarrow {}^7F_2/{}^5D_0 \rightarrow {}^7F_1$) is 2.06, indicating a low symmetry for the electrostatic field surrounding Eu(III) [40]. It could be seen from Fig. 3 that in acetone solution the Eu(III) complex has the strongest luminescence, and then in acetonitrilet, $CHCl_3$, DMF and DMSO. This is due to the coordinating effects of solvents, namely, solvate effect [40]. Together with the raising coordination abilities of acetone, acetonitrilet, DMF and DMSO

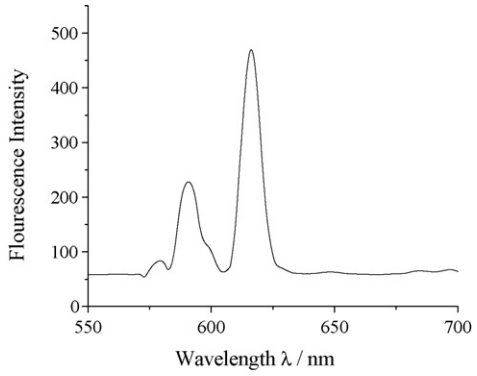

Fig. 2. Emission spectrum of the Eu(III) complex in solid state at room temperature.

for the lanthanide ions, the oscillatory motions of the entering molecules consume more energy which the ligand triplet level transfer to the emitting level of the lanthanide ion. Thus, the energy transfer could not be carried out perfectly.

3.5. Electronic absorption titration

Before reacting complexes **1** and **2** with DNA, the interactions of free Sm and Eu cations with DNA was checked by UV/vis titration of DNA. It should be stressed that under experimental conditions (pH 7.1, $c(Ln^{3+}) = 1 \times 10^{-5}$ M), Sm(III) and Eu(III) ion itself does not show any measurable interactions with studied DNA.

Electronic absorption spectroscopy is one of the most powerful experimental techniques for probing metal ion–DNA interactions. Binding of the macromolecule leads to changes in the electronic spectrum of the metal complex. Base binding is expected to perturb the ligand field transition of the metal complex. Intercalative mode of binding usually results in hypochromism and bathochromism due to the strong stacking interaction between an aromatic chromophore and the base pairs of DNA. The extent of hypochromism parallels the intercalative binding strength [41,42]. On the other hand, metal complexes, which bind non-intercalatively or electrostatically with DNA may result in hyperchromism or hypochromism.

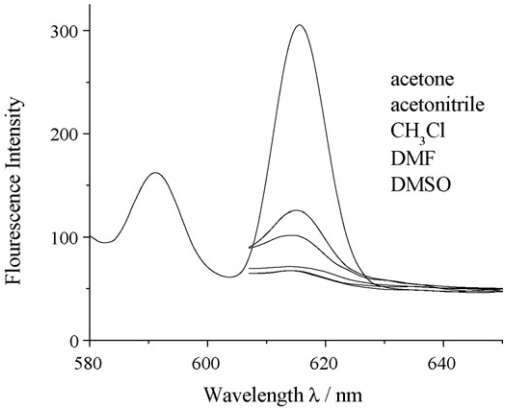

Fig. 3. Emission spectra of the Eu(III) complex in different solutions at room temperature.

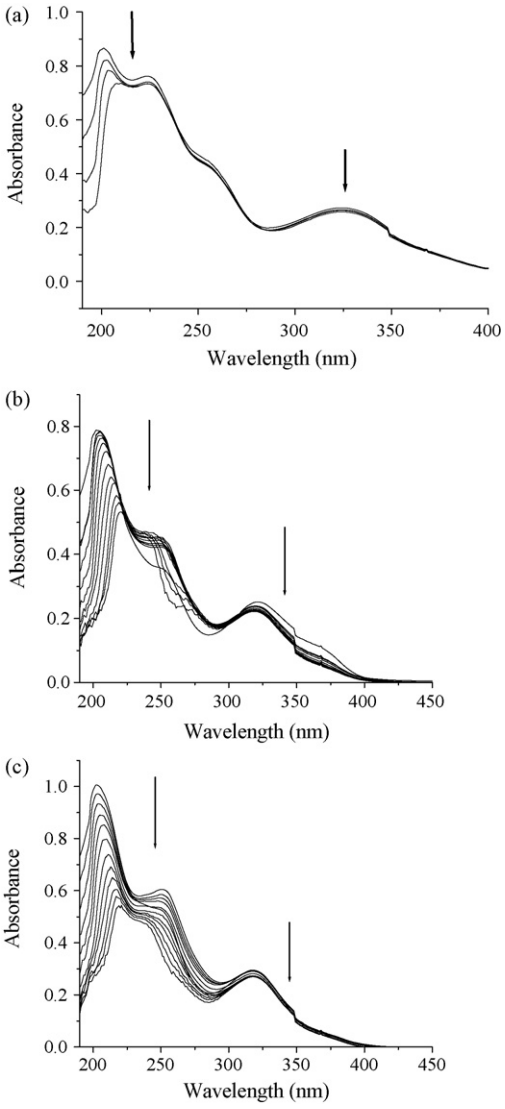

Fig. 4. (a) Electronic spectra of ligand (10 μM) in the presence of increasing amounts of CT-DNA. [DNA] = 0–10 μM. Arrow shows the absorbance changes upon increasing DNA concentration. (b) Electronic spectra of Sm(III) complex (10 μM) in the presence of increasing amounts of CT-DNA. [DNA] = 0–55 μM. Arrow shows the absorbance changes upon increasing DNA concentration. (c) Electronic spectra of Eu(III) complex (10 μM) in the presence of increasing amounts of CT-DNA. [DNA] = 0–55 μM. Arrow shows the absorbance changes upon increasing DNA concentration.

The absorption spectra of Sm(III) and Eu(III) complexes, and ligand (**L**) in the absence or presence of CT-DNA are given in Fig. 4. For the Sm(III) complex, the intensity of the intraligand band at 204 nm decreases with increasing concentration of DNA. Addition of DNA also leads to changes in the position of absorption bands. The 204 nm band is red shifted by 17 nm in the presence of DNA. In the case of complex **2** also, the intensity of the intraligand band at 203 nm markedly decreases and the 203 nm band is red shifted by 17 nm in the presence of DNA. Free ligand at 200 nm exhibits hypochromism, and bathochromism of about 7 nm. For two complexes, the band at 250 nm is hypsochromic shift, and the intensity of the band at 320 nm has no obvious decrease and maxima shift. These results suggest

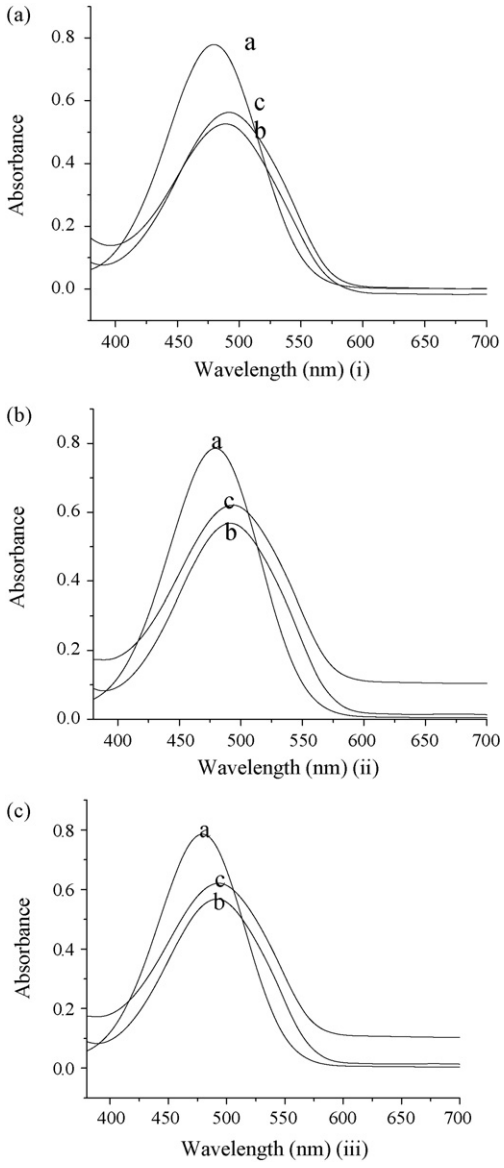

Fig. 5. (i) Free ligand (**L**); (ii) complex **1** and (iii) complex **2**. The visible absorption spectra of (a) 1×10^{-5} M EB; (b) a + 1×10^{-4} M DNA; (c) b + 1×10^{-5} M of compound in Tris–HCl buffer (5 mM Tris–HCl, 50 mM NaCl, pH 7.1) solution.

an intimate association of the compounds with CT-DNA. However, we cannot confirm that two complexes bind to DNA via intercalation.

In order to test if the compounds bind to DNA via intercalation, ethidium bromide (EB) was employed, as EB interacts with DNA as a typical indicator of intercalation [43]. Fig. 5a shows that the maximal absorption of EB at 479 nm decreased and shifted to 515 nm in the presence of DNA, Fig. 7b, which is characteristic of intercalation. Fig. 5c(i–iii) is the absorption of a mixture solution of EB, the compounds and DNA.

It was found that the absorption at 515 nm increased; Fig. 5c(i–iii) compared with Fig. 5b(i–iii) for all the compounds tested (i) **L**, (ii) **1**, (iii) **2**. This could result from two reasons: (1) EB bound to the compounds strongly, resulting in a decreased amount of EB intercalated into DNA; (2) there exists competitive intercalation between the compounds and EB with DNA, thus, releasing some free EB from the DNA–EB system. The former reason can be precluded since there were no new absorption peaks.

3.6. Fluorescence spectra studies

The fluorescence Scatchard plot has been confirmed to be effective for characterizing the binding mode of the metal complexes to DNA [44–46]. The enhancements in the emission intensity of the complexes **1** and **2**, and ligand with increasing CT-DNA concentrations are shown in Fig. 6. In the absence of DNA, **1** and **2**, and ligand emit weak luminescence in Tris buffer at ambient temperature, with a maximum appearing at 449 nm. When DNA is present the intensity of the emission for complexes **1** and **2**, and ligand all increase with respect to DNA concentration. This phenomenon is related to the extent to which the compounds penetrate into the hydrophobic environment inside the DNA, thereby avoiding the quenching effect of solvent water molecules. The binding of complexes **1** and **2**, and ligand to CT-DNA leads to a marked increase in the emission intensity, which also agrees with those observed for other intercalators [24,26,30]. According to the Scathchard equation, a plot of r/C_f versus r gave the binding constants 9.28×10^6, 8.40×10^6 and 4.88×10^6 M^{-1} from the fluorescence data for complexes **1** and **2**, and ligand, respectively. This value is similar to the one reported for some flavane benzoyl hydrazones like Eu(III) ($K_b = 3.55 \times 10^6$ M^{-1}) and La(III) ($K_b = 1.83 \times 10^7$ M^{-1}) complexes [24,26].

The DNA-binding modes of three compounds were further monitored by a fluorescent EB displacement assay. It is well known that EB can intercalate nonspecifically into DNA which causes it to fluoresce strongly. Competitive binding of other drugs to DNA and EB will result in displacement of bound EB and a decrease in the fluorescence intensity. This fluorescence-based competition technique can provide indirect evidence for the DNA-binding mode. Fig. 7 shows the emission spectra of DNA–EB system with increasing amounts of the complexes **1** and **2**, and ligand. The emission intensity of the DNA–EB system ($\lambda_{em} = 582$ nm) decreased apparently as the concentration of the complexes **1** and **2**, and ligand increased, and an isobathic point appeared at 536 nm or so for complexes **1** and **2**. The quenching plots illustrate that the quenching of EB bound to DNA by the compounds is in good agreement with the linear Stern–Volmer equation. The emission band at 584 nm of the DNA–EB system decreased in intensity with an increase in the concentration of the two compounds, which indicated that the compounds could displace EB from the DNA–EB system. The resulting decrease in fluorescence was caused by EB changing from a hydrophobic environment to an aqueous environment [47]. Such a characteristic change is often observed in intercalative DNA interactions [23,24,26,48]. The quenching plots illustrate that the quenching of EB bound to DNA by the complexes is in good agreement with the linear Stern-Volmer equation. In the plots of F_0/F versus $[Q]$, K_q is given by the ratio of the slope to the intercept. The K_q values for the complexes **1** and **2**, and ligand are 1.20×10^5, 1.64×10^4 and 2.26×10^3,

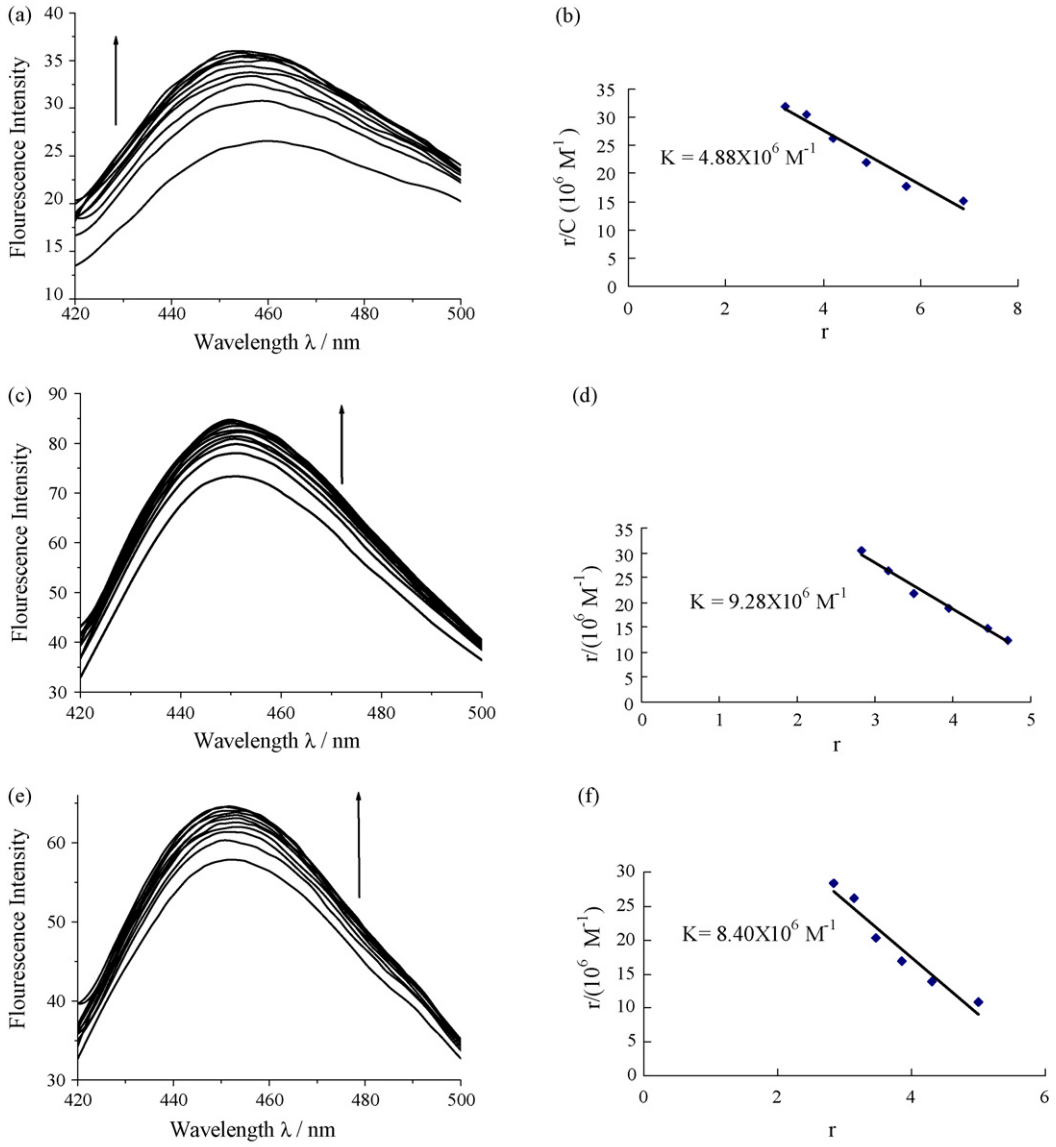

Fig. 6. (a) The emission enhancement spectra of ligand (10 μM) in the presence of 0, 0.4, 0.8, 1.2, 1.6, 2.0, 2.4, 2.8, 3.2, 3.6 and 4.0 μM CT-DNA. Arrow shows the emission intensities changes upon increasing DNA concentration. Inset (b): Scatchard plot of the fluorescence titration data of ligand, $K = 4.88 \times 10^6\ M^{-1}$. (c) The emission enhancement spectra of Sm(III) complex (10 μM) in the presence of 0, 0.4, 0.8, 1.2, 1.6, 2.0, 2.4, 2.8, 3.2, 3.6 and 4.0 μM CT-DNA. Arrow shows the emission intensities changes upon increasing DNA concentration. Inset (d): Scatchard plot of the fluorescence titration data of ligand, $K = 9.28 \times 10^6\ M^{-1}$. (e) The emission enhancement spectra of Eu(III) complex (10 μM) in the presence of 0, 0.4, 0.8, 1.2, 1.6, 2.0, 2.4, 2.8, 3.2, 3.6 and 4.0 μM CT-DNA. Arrow shows the emission intensities upon increasing DNA concentration. Inset (f): Scatchard plot of the fluorescence titration data of Eu(III) complex, $K = 8.40 \times 10^6\ M^{-1}$.

respectively. The binding constants were also calculated using following Eq. (1) [49]:

$$C_{\mathrm{Eth}} = 2(F^0 - F)\frac{E_t}{F^0}$$

$$r_{\mathrm{Eth}} = \frac{E_t - C_{\mathrm{Eth}}}{C_{\mathrm{DNA}}}$$

$$r_M = \frac{n - r_{\mathrm{Eth}} - r_{\mathrm{Eth}}}{K_{\mathrm{Eth}} C_{\mathrm{Eth}}}$$

$$C_M = M_t - r_M C_{\mathrm{DNA}}$$

$$K_M = \frac{[(n - r_{\mathrm{Eth}})K_{\mathrm{Eth}}(C_{\mathrm{Eth}}/r_{\mathrm{Eth}}) - 1]}{C_M}$$

where F is observed fluorescence emission intensity of DNA–EB system; F the intensity in the absence of compound; E_t the total EB concentration; C_{Eth} the free EB concentration; C_M the bound compound concentration, and M_t is the total compound concentration. From above equation, the binding constants of complexes **1** and **2**, and ligand are 8.98×10^6, 8.12×10^6 and $4.58 \times 10^6\ M^{-1}$, respectively. These values are almost equal to the binding constants determined by the fluorescence titration experiments, so we can conclude that the quenching of DNA–EB system is due to the displacement of EB upon binding of the complexes or ligand.

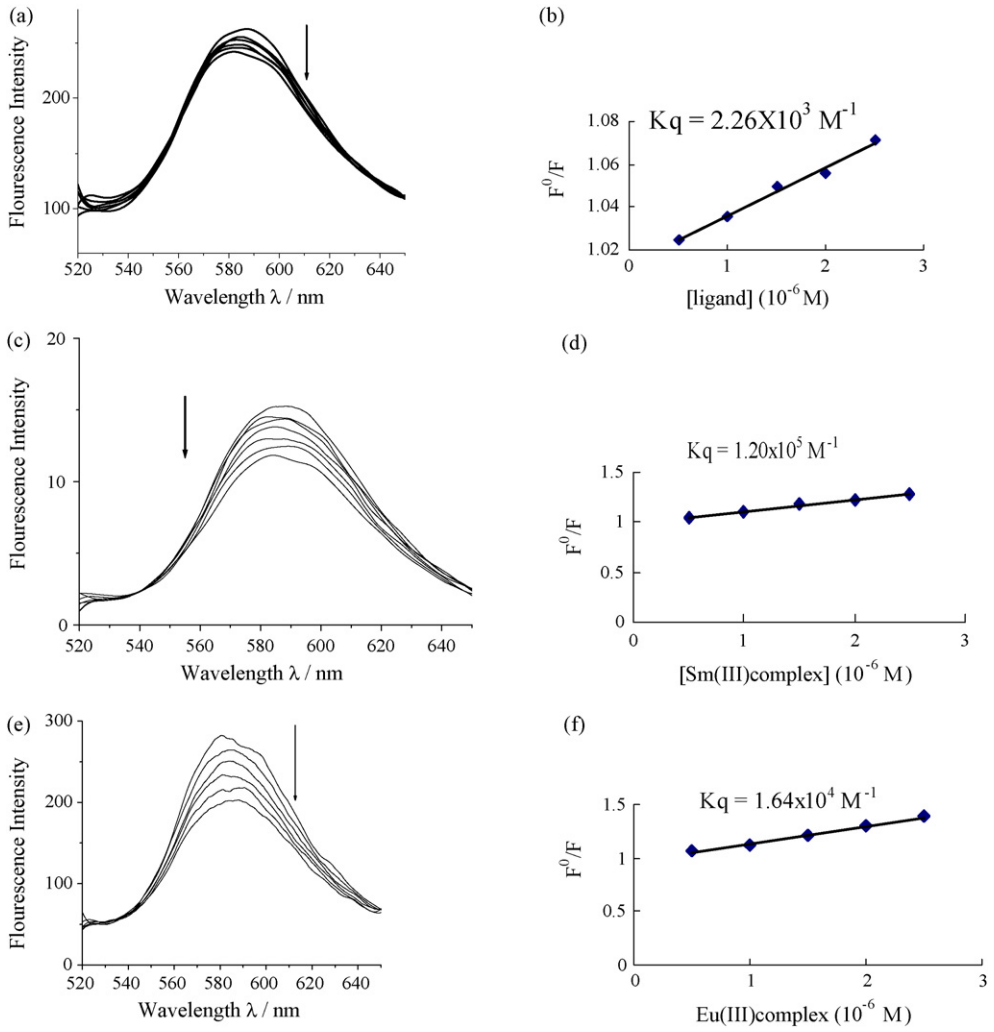

Fig. 7. (a) The emission spectra of DNA–EB system (10 and 0.32 μM EB), λ_{ex} = 500 nm, λ_{em} = 520.0–650.0 nm, in the presence of 0, 5, 10, 15, 20, 25 μM ligand. Arrow shows the emission intensities changes upon increasing ligand concentration. Inset (b): Stern–Volmer plot of the fluorescence titration data of ligand, $K_q = 2.26 \times 10^3\ M^{-1}$. (c) The emission spectra of DNA–EB system (10 and 0.32 μM EB), λ_{ex} = 500 nm, λ_{em} = 520.0–650.0 nm, in the presence of 0, 5, 10, 15, 20, 25 μM Sm(III) complex. Arrow shows the emission intensities changes upon increasing Sm(III) complex concentration. Inset (d): Stern–Volmer plot of the fluorescence titration data of Sm(III) complex, $K_q = 1.20 \times 10^5\ M^{-1}$. (e) The emission spectra of DNA–EB system (10 and 0.32 μM EB), λ_{ex} = 500 nm, λ_{em} = 520.0–650.0 nm, in the presence of 0, 5, 10, 15, 20, 25 μM Eu(III) complex. Arrow shows the emission intensities changes upon increasing Eu(III) complex concentration. Inset (f): Stern–Volmer plot of the fluorescence titration data of Eu(III) complex, $K_q = 1.64 \times 10^4\ M^{-1}$.

3.7. Viscosity measurements

Optical photophysical probes provide necessary, but not sufficient evidence to support the mode of binding of metal complexes with DNA. The viscosity of a DNA solution is sensitive to the addition of metal complexes which can bind to DNA. While intercalation leads to increase in viscosity because the DNA base pairs are pushed apart to accommodate the bound ligand, a partial, non-classical mode of binding could bend or kink the DNA helix, reduces its effective length and thereby its viscosity. To further confirm the interaction mode of the Ln(III) complexes with DNA, a comparative viscosity study between the EB and the two complexes were carried out (Fig. 8). The effects of the compounds together with EB on the viscosity of DNA are shown in Fig. 8. It is found that the viscosity of DNA increases steadily with the increase of the concentration of the compounds, which is similar to that of a classical intercalator EB [50]. This result demonstrates that the complexes and EB bind to DNA through the same way, i.e., the classical intercalation mode, which also parallels the pronounced hypochromism and spectral red shift of the complex in the absorption spectrum experiment.

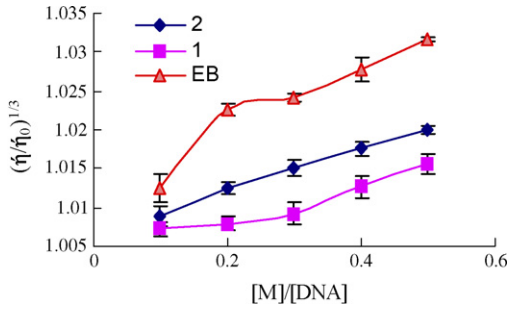

Fig. 8. Effect of increasing amounts of complexes **1** and **2**, and EB on the relative viscosity of calf thymus DNA at 25.0 °C.

Table 2
Inhibition effect against HepG2 cell lines

Compounds	Average inhibition effect (%)		
	C_1[a]	C_2[a]	C_3[a]
Ligand	58.26 ± 1.80	67.63 ± 2.68	93.25 ± 0.48
Complex **3**	20.45 ± 1.25	21.35 ± 1.56	54.54 ± 1.09
Complex **1**	39.26 ± 1.24	46.42 ± 0.86	61.84 ± 2.42
Complex **2**	43.66 ± 0.86	54.95 ± 1.24	65.98 ± 3.2

Date are expressed as mean ± S.D. ($n = 3$).
[a] C_i was concentration: $C_{i(i=1-3)} = 0.0625, 1.25, 2.5$ μM.

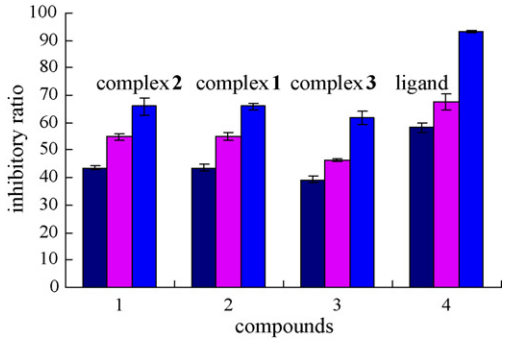

Fig. 9. Cytotoxic activity of compounds against HepG2.

3.7.1. *In vitro cytotoxicity*

The cytotoxicity assays of complexes and ligand **L** against HepG2 cancer cell lines were listed in Table 2. As shown in Table 2, the average inhibitory ratio against HepG2 cancer cell lines increases with the increase of the concentration in the range of the tested concentration (see Fig. 9). The Eu(III) complex is the most effective in the three complexes against HepG2 cancer cell lines, whereas, the La(III) complex has the poorest inhibitory. It is clear that nature of the rare earth ions affect the ability that the complex inhibits the cancer cell lines. The ligand has a higher inhibitory effect than the complexes do. The cytotoxic activities are not in accord with the experimental results. It will be further studied.

4. Conclusion

Taken together, a new ligand, ethylenediiminobi(6-hydroxychromone-3-carbaldehyde) Schiff-base (L), and its Ln(III) complexes have been prepared and characterized. The DNA-binding properties of complexes **1** and **2** were investigated by absorption, fluorescence and viscosity measurements. The results support the fact that the compounds bind to CT-DNA via intercalation. All compounds showed certain cytotoxic activity against HepG2 cancer cell lines. These findings clearly indicate that lanthanide-based complexes have many potential practical applications, like the development of nucleic acid molecular probes and new therapeutic reagents for diseases.

Acknowledgements

This work is supported by the National Natural Science Foundation of China (20475023).

References

[1] M.J. Waring, in: G.C.K. Roberts (Ed.), Drug Action at the Molecule Level, Macmillan, London, 1977, p. 167.
[2] G.M. Zhang, S.M. Shuang, C. Dong, D.S. Liu, M.M.F. Choi, J. Photochem. Photobiol. B 74 (2004) 127.
[3] C. Li, S.L. Liu, L.H. Guo, D.P. Chen, Electrochem. Commun. 7 (2005) 23.
[4] R.Y. Zhang, D.W. Pang, R.X. Cai, Chem. J. Chin. Univ. 20 (1999) 1210.
[5] C.M. Dupureur, J.K. Barton, Inorg. Chem. 36 (1997) 33–43.
[6] I. Greguric, J.R. Aldrich-Wright, J.G. Collins, J. Am. Chem. Soc. 119 (1997) 3621–3622.
[7] R.B. Nair, E.S. Teng, S.L. Kirkland, C.J. Murphy, Inorg. Chem. 37 (1998) 139–141.
[8] J.G. Liu, B.H. Ye, H. Li, L.N. Ji, R.H. Li, J.Y. Zhou, J. Inorg. Biochem. 3 (1999) 117–122.
[9] B. Onfelt, L. Gostring, P. Lincoln, B. Nordén, A. Onfelt, Mutagenesis 17 (2002) 317–320.
[10] P. Knekt, R. Jarvinen, R. Seppanen, M. Heliovaara, L.T. Pukkala, A. Aromaa, Am. J. Epidemiol. 146 (1997) 223–230.
[11] Y. Sakaguchi, Y. Maehara, H. Baba, T. Kusumoto, K. Sugimachi, R.A. Newmanv, Cancer Res. 52 (1992) 3306–3309.
[12] S. Habtemariam, J. Nat. Prod. 60 (1997) 775–778.
[13] I. Aljancic, V. Vajs, N. Menkovic, I. Karadzic, N. Juranic, S. Milosavljevic, S. Macura, J. Nat. Prod. 62 (1999) 909–911.
[14] F. Ko, C. Chu, C. Lin, C. Chang, C. Teng, Biochim. Biophys. Acta 1389 (1998) 81–90.
[15] A. Nkengfack, T. Vouffo, Z. Fomun, M. Meyer, S.O. Bergendorff, Phytochemistry 36 (1994) 1047–1051.
[16] Z.M. Wang, H.K. Lin, S.R. Zhu, T.F. Liu, Z.F. Zhou, Y.T. Chen, Anti-Cancer Drugs Des. 15 (2000) 405.
[17] F.H. Lia, G.H. Zhao, H.X. Wu, H. Lin, X.X. Wu, S.R. Zhu, H.K. Lin, J. Inorg. Biochem. 100 (2006) 36–43.
[18] H.X. Xu, H.Y. Zhang, X.G. Qu, J. Inorg. Biochem. 100 (2006) 1646–1652.
[19] A. Cha, G.E. Snyder, P.R. Selvin, F. Bezanilla, Nature 402 (1999) 809–813.
[20] P. Caravan, J. Ellison, T. McMurry, R. Lauffer, Chem. Rev. 99 (1999) 2293–2352.
[21] K. Wang, R. Li, Y. Cheng, B. Zhu, Coord. Chem. Rev. 192 (1999) 297–308.
[22] M. Marinić, I. Piantanida, G. Rusak, M. Žinić, J. Inorg. Biochem. 100 (2006) 288–298.
[23] Z.Y. Yang, B.D. Wang, Y.H. Li, J. Organometal. Chem. 691 (2006) 4156–4166.
[24] B.D. Wang, Z.Y. Yang, T.R. Li, Bioorg. Med. Chem. 14 (2006) 6012–6021.
[25] B.D. Wang, Z.Y. Yang, Y. Wang, Synth. React. Inorg. Met-Org. Nano-Met. Chem. 35 (2005) 533–539.
[26] B.D. Wang, Z.Y. Yang, Q. Wang, T.K. Cai, P. Crewdson, Bioorg. Med. Chem. 14 (2006) 1880–1888.
[27] J. Marmur, J. Mol. Biol. 3 (1961) 208.
[28] C.V. Kumar, E.H. Asuncion, J. Am. Chem. Soc. 115 (1993) 8547–88553.
[29] B.D. Wang, Z.Y. Yang, D.W. Zhang, Y. Wang, Spectrochim. Acta Part A 63 (2006) 213–219.
[30] S. Satyanarayana, J.C. Dabrowiak, J.B. Chaires, Biochemistry 31 (1992) 9319–9324.
[31] G.M. Howe, K.C. Wu, W.R. Bauer, Biochemistry 19 (1976) 339–347.
[32] C.V. Kumar, J.K. Barton, M.J. Turro, J. Am. Chem. Soc. 107 (1985) 5518–5523.
[33] J.K. Barton, A.T. Danishefsky, J.M. Golderg, J. Am. Chem. Soc. 106 (1984) 2172–2176.
[34] M.R. Efink, C.A. Ghiron, Anal. Biochem. 114 (1981) 199–206.
[35] M. Eriksson, M. Leijon, C. Hiort, B. Norden, A. Gradsland, Biochemistry 33 (1994) 5031–5040.
[36] T.C. Michael, R. Marisol, J.B. Allen, J. Am. Chem. Soc. 111 (1989) 8901–8911.
[37] M.R. Eftink, G.C.A. hiron, Anal. Biochem. 114 (1981) 199.
[38] W.J. Geary, Coord. Chem. Rev. 7 (1971) 1–122.
[39] F.D. Lewis, S.V. Barancyk, J. Am. Chem. Soc. 111 (1989), 8653–865161.
[40] M. Albin, R.R. Wright Jr., W.D. Horrochs, Inorg. Chem. 24 (1985) 2491.
[41] J.K. Barton, J.J. Dannenberg, A.L. Raphael, J. Am. Chem. Soc. 106 (1984) 2172–2176.

[42] V.A. Bloomfield, D.M. Crothers, I. Tinoco, Physical Chemistry of Nucleic Acids, Harper and Row, New York, 1974, p. 432.
[43] D.L. Boger, B.E. Frink, S.R. Brunette, W.C. Tse, M.P. Hedrick, J. Am. Chem. Soc. 123 (2001) 5878.
[44] M. Howe-Grant, K.C. Wu, W.R. Bauer, S.J. Lippard, Biochemistry 15 (1976) 4339.
[45] G. Zhao, H. Lin, S. Zhu, H. Sun, Y. Chen, J. Inorg. Biochem. 70 (1998) 219.
[46] Z.M. Wang, S.R. Zhu, H.K. Lin, M. Xu, T.F. Liu, S. Zhu, H. Sun, Y.T. Chen, Acta Chim. Sinica. 59 (2001) 701.
[47] Y.B. Zeng, N. Yang, W.S. Liu, N. Tang, J. Inorg. Biochem. 97 (2003) 258–264.
[48] C.V. Kumar, J.K. Barton, N.J. Turro, J. Am. Chem. Soc. 107 (1985) 5518.
[49] C.G. Reinhardt, T.R. Krugh, Biochemistry 17 (1978) 4845.
[50] X.L. Wang, H. Chao, H. Li, X.L. Hong, Y.J. Liu, L.F. Tan, L.N. Ji, J. Inorg. Biochem. 98 (2004) 1143.